Eigenvalue Beamforming using a Multi-rank MVDR Beamformer

Louis Scharf, Colorado State University, Fort Collins, CO 80523, scharf@engr.colostate.edu
Ali Pezeshki, Princeton University, Princeton, NJ 08544, pezeshki@princeton.edu
Barry Van Veen, University of Wisconsin, Madison, WI 53706, vanveen@engr.wisc.edu
Henry Cox, Lockheed Martin, Arlington, VA 22203, harry.cox@lmco.com
Olivier Besson, ENSICA, Toulouse, France, besson.vincent@ensica.fr

***Abstract*— We derive multi-rank generalizations of the MVDR beamformer to separate an unknown signal of interest in the presence of interference and noise. The spatial signature of the signal is assumed to lie in a known linear subspace, but the orientation of the signal in that subspace is otherwise unknown. The unknown orientation may be fixed for a sequence of experimental realizations, in which case the signal has a rank-1 covariance matrix, or it may be random over realizations, in which case the signal covariance is multi-rank. We derive two generalizations of the MVDR beamformer: a *matched direction beamformer*, for the rank-1 case where the signal is drawn from an unknown but fixed direction within a known multi-dimensional subspace, and a *matched subspace beamformer*, for the multi-rank case where the signal is drawn from a known multi-dimensional subspace.**

I. Introduction

In many applications of radar and sonar it is desired to separate a signal of interest in the presence of interference and noise using measurements from L sensor elements, e.g. see [1]. Typically, the problem is one of estimating a signal $s(t)$ or its power in the measurement model

$$\mathbf{x}(t) = \mathbf{s}(t) + \boldsymbol{\nu}(t) + \mathbf{n}(t); \quad \mathbf{s}(t) = \mathbf{a}s(t), \tag{1}$$

where $\mathbf{a}$ is the signature of interest, $\boldsymbol{\nu}(t)$ is the interference vector, and $\mathbf{n}(t)$ is broadband noise.

In most situations, the signature vector $\mathbf{a}$ is not perfectly known, due to factors such as multi-path, local and random scattering, near field wavefront formation, random fluctuations in the propagation medium, flexing arrays, array calibration errors, uncertainty about the direction of arrival (DOA) of the source, and movement of the source. Differences between the presumed signature and the actual signature result in signal suppression and poor interference rejection, degrading the performance of adaptive beamformers (e.g. see [2]).

We derive two *multi-rank* generalizations of the MVDR beamformer, namely a *matched direction beamformer* and a *matched subspace beamformer*, to separate an unknown signal of interest, assuming that some knowledge about its signature vector is available. We assume that the signature vector $\mathbf{a}$ lies in a known linear subspace but its direction, or orientation, within the subspace is unknown. The unknown orientation may stand up over a sequence of experimental realizations, in which case the signal covariance matrix is rank-one. Or the unknown orientation may change from realization to realization, in which case the signal covariance is multi-rank.

The idea for deriving both beamformers is to ask for a designed response to the signal subspace while minimizing the power at the output of the beamformer. We show that multi-rank beamformers may be designed by using a multi-rank MVDR beamformer or its equivalent generalized sidelobe canceller (GSC), followed by a resolution onto a dominant subspace (for matched direction beamforming) or a subdominant subspace (for matched subspace beamforming). The eigenvalues of the error covariance matrix associated with LMMSE estimation in the GSC play a key role in resolving signals of interest. The dominant eigenvalues of the error covariance matrix resolve signals with rank-1 covariances and the subdominant eigenvalues resolve signals with multi-rank covariances. Thus, the beamformers we advocate may be viewed as eigenvalue beamformers. But, more importantly, it is eigenvalues of an error covariance, or beamformed covariance, that matter- not eigenvalues of measurement covariance matrices. Numerical examples are presented to demonstrate the performance of eigenvalue beamforming. The work that laid the foundation for this paper is reported in [3].

II. Signal Models

Consider the general L-dimensional data model (1). Assuming that $\mathbf{s}$, $\mathbf{v}$, and $\mathbf{n}$ are uncorrelated and have zero means, we may express the measurement covariance matrix as

$$\mathbf{R} = E[\mathbf{x}\mathbf{x}^H] = \mathbf{R}_{ss} + \mathbf{R}_{\nu\nu} + \mathbf{R}_{nn}, \tag{2}$$

where $\mathbf{R}_{ss} = \mathbf{E}[\mathbf{s}\mathbf{s}^H]$ is the signal covariance, $\mathbf{R}_{\nu\nu} = \mathbf{E}[\boldsymbol{\nu}\boldsymbol{\nu}^H]$ is the interference covariance, and $\mathbf{R}_{nn} = \mathbf{E}[\mathbf{n}\mathbf{n}^H] = \sigma_n^2\mathbf{I}$ is the noise covariance. We assume that the signal $\mathbf{s}$ lies in a linear subspace and consider the two following signal models.

Model 1: Standing waves from a known p-dimensional subspace. The signal (wavefront) model is

$$\mathbf{s} = \boldsymbol{\Psi}\mathbf{b}_o s, \tag{3}$$

where $\boldsymbol{\Psi}$ is a known $L \times p$ ($p < L$) matrix with orthonormal columns, spanning a p-dimensional subspace $\langle\boldsymbol{\Psi}\rangle$. The vector $\mathbf{b}_o$ is an *unknown but fixed* $p \times 1$ unit-norm complex vector that determines the orientation of $\mathbf{s}$ in $\langle\boldsymbol{\Psi}\rangle$, and s is a zero-mean random complex amplitude with variance $\sigma_s^2 = E[ss^\star]$. Here, the signal $\mathbf{s}$ is known to lie inside the p-dimensional

subspace $\langle \mathbf{\Psi} \rangle$ but the coordinates of $\mathbf{s}$ in $\langle \mathbf{\Psi} \rangle$ are unknown. The signal $\mathbf{s}$ has a rank-1 covariance matrix for the form

$$\mathbf{R}_{ss} = E[\mathbf{s}\mathbf{s}^H] = \sigma_s^2 \mathbf{\Psi} \mathbf{b}_o \mathbf{b}_o^H \mathbf{\Psi}^H. \quad (4)$$

Here, the relative phasings and amplitudes induced by the signal on the array elements do not vary from snapshot to snapshot, as all the realizations of $\mathbf{s}$ are built from the same linear combination of the columns of $\mathbf{\Psi}$. All the wavefronts in a sequence of snapshots have the same "shape", hence the name standing waves.

The model (3) is applicable when there is deterministic uncertainty about the signature vector, due to uncertainty in the exact source direction or due to array calibration errors. This model is also relevant in slow-varying multi-path scenarios, where the signal $\mathbf{s}$ is a superposition of waves arriving from different angles (paths) and path gains are unknown but fixed during the observation interval.

Model 2: Fluctuating waves from a known p-dimensional subspace. The signal (wavefront) model is

$$\mathbf{s} = \mathbf{\Psi} \mathbf{b} s, \quad (5)$$

where $\mathbf{\Psi}$ is a known $L \times p$ ($p < L$) matrix with orthonormal columns, spanning a p-dimensional subspace $\langle \mathbf{\Psi} \rangle$. The vector $\mathbf{b}$ is a $p \times 1$ zero-mean complex random vector with rank-p covariance $\mathbf{R}_{bb} = E[\mathbf{b}\mathbf{b}^H]$, normalized so that $\mathrm{tr}\{\mathbf{R}_{bb}\} = 1$, and s is a random complex amplitude with variance σ_s^2 independent of $\mathbf{b}$. Consequently, the signal $\mathbf{s}$ has a rank-p covariance matrix of the form

$$\mathbf{R}_{ss} = E[\mathbf{s}\mathbf{s}^H] = \sigma_s^2 \mathbf{\Psi} \mathbf{R}_{bb} \mathbf{\Psi}^H. \quad (6)$$

The relative phasings and amplitudes induced by the signal on the array elements vary from snapshot to snapshot, as each realization of $\mathbf{s}$ is built from a different linear combination of the columns of $\mathbf{\Psi}$. Each wavefront in a sequence of snapshots has a different shape, hence the name fluctuating waves.

The model (5) is applicable when $\mathbf{s}$ is produced by a distributed source. It is also applicable when the uncertainty in the signature vector changes randomly during the observation interval, e.g., due to a flexing of a towed array in sonar.

Remark. For a narrowband but spatially distributed source which radiates towards an L-element uniform linear array (ULA) with angular power density $S(\theta) = 1$, $\theta \in [\theta_o - \beta\pi, \theta_o + \beta\pi]$, $0 \leq \beta \leq 1$ the numerical rank of $\mathbf{R}_{ss}$ is $p \approx \beta L$, and $\mathbf{\Lambda} \approx \frac{1}{p}\mathbf{I}$. In such a case, the columns of $\mathbf{\Psi}$ are the first p discrete prolate spheroidal wave functions (DPSWFs) and $\langle \mathbf{\Psi} \rangle$ is the corresponding $p-$dimensional *Slepian subspace* [4].

III. Multi-Rank MVDR Beamforming

The idea in standard MVDR is to design a vector beamformer $\mathbf{w}$ to minimize the output power $E[yy^H] = E[(\mathbf{w}^H\mathbf{x})(\mathbf{w}^H\mathbf{x})^H]$ under the constraint that the beamformer produces a unit-magnitude response $\mathbf{w}^H\boldsymbol{\psi} = q$, $|q|^2 = 1$ to a waveform with a *known* signature vector $\mathbf{a} = \boldsymbol{\psi}$. For signals of the form (3) and (5) the signature vector is not known, but the subspace $\langle \mathbf{\Psi} \rangle$ in which the signature lies is known. In this case, it seems more natural to design a *matrix beamformer* $\mathbf{W} = [\mathbf{w}_1, \mathbf{w}_2, \ldots \mathbf{w}_r] \in \mathbb{C}^{L \times r}$ and to ask for a designed response in the subspace $\langle \mathbf{\Psi} \rangle$. Thus, we constrain the matrix beamformer $\mathbf{W}$ to satisfy the subspace constraint

$$\mathbf{W}^H \mathbf{\Psi} = \mathbf{Q}^H, \quad (7)$$

where $\mathbf{Q}$ is a $p \times r$ ($r \leq p$) left-orthogonal matrix, i.e. $\mathbf{Q}^H\mathbf{Q} = \mathbf{I}_{r \times r}$ and $\mathbf{Q}\mathbf{Q}^H = \mathbf{P}_{\mathbf{Q}}$, an orthogonal projection onto $\langle \mathbf{Q} \rangle$. This subspace constraint is equivalent to $\mathbf{W}^H\mathbf{\Psi}\,[\mathbf{Q}\ \ \mathbf{Q}_\star] = [\mathbf{I}\ \ \mathbf{0}]$, where $[\mathbf{Q}\ \ \mathbf{Q}_\star] \in \mathbb{C}^{p \times p}$ is an orthogonal matrix. This shows that under the constraint in (7) $\mathbf{W}^H$ images the r linear combinations (or vectors) $\mathbf{\Psi}\mathbf{Q}$ as $\mathbf{I}$ and the $p - r$ linear combinations $\mathbf{\Psi}\mathbf{Q}_\star$ as zero. These may be called *distortionless* and *zero-forcing* constraints, respectively. The question that naturally arises here is: how should the constraint vectors $\mathbf{\Psi}[\mathbf{Q}\ \ \mathbf{Q}_\star]$, or equivalently the left-orthogonal constraint matrix $\mathbf{Q}$, be designed? We defer the answer to this question until Section V. Until then, we assume that $\mathbf{Q}$ is a known left-orthogonal matrix.

A natural beamforming strategy would be to design $\mathbf{W}$ to minimize the output power $\mathrm{tr}\{E[\mathbf{y}\mathbf{y}^H]\} = \mathrm{tr}\{\mathbf{W}^H\mathbf{x}\mathbf{x}^H\mathbf{W}\}$, while forcing the subspace constraint in (7):

$$\min_{\mathbf{W} \in \mathbb{W}} P = \mathrm{tr}\{\mathbf{W}^H\mathbf{R}\mathbf{W}\} \quad \text{u.c.} \quad \mathbf{W}^H\mathbf{\Psi} = \mathbf{Q}^H. \quad (8)$$

This may be viewed as a *multi-rank* generalization of the standard MVDR beamformer, as it yields a matrix minimum variance beamformer $\mathbf{W}^H$, under designed distortionless and zero-forcing constraints in a *multi-dimensional* subspace. We note that multi-rank beamforming problems of the form (8) have been considered in [5]–[7]. What distinguishes our work is that in [5]–[7] the constraint matrix $\mathbf{Q}$ is pre-specified, whereas in this paper we design the constraint matrix $\mathbf{Q}$.

The solution to (8) is

$$\mathbf{W}_o = \mathbf{R}^{-1}\mathbf{\Psi}(\mathbf{\Psi}^H\mathbf{R}^{-1}\mathbf{\Psi})^{-1}\mathbf{Q}, \quad (9)$$

$$P_o = \mathrm{tr}\{\mathbf{W}_o^H\mathbf{R}\mathbf{W}_o\} = \mathrm{tr}\{\mathbf{Q}^H(\mathbf{\Psi}^H\mathbf{R}^{-1}\mathbf{\Psi})^{-1}\mathbf{Q}\}. \quad (10)$$

We call the $L \times r$ matrix $\mathbf{W}_o$ a *rank$-r$ MVDR or Capon beamformer*. It is important to note that the matrix $\mathbf{\Psi}$ in (8) is steered to a particular bearing or electrical angle, as the subspace in which the signal lies depends on the spatial location of the source. Therefore, the minimization problem in (8) has to be solved for every electrical angle of interest. Naturally, the multi-rank MVDR beamformer $\mathbf{W}_o$ and the output power P_o are functions of electrical angle, by virtue of their dependence on $\mathbf{\Psi}$. For this reason, the plot of the output power P_o versus electrical angle may be called the *multi-rank MVDR bearing response pattern*.

IV. Generalized Sidelobe Canceller

The multi-rank beamformer in (9) may be expressed as $\mathbf{W}_o = [\mathbf{\Psi} - \mathbf{G}\mathbf{F}]\mathbf{Q}$, where $\mathbf{F} = (\mathbf{G}^H\mathbf{R}\mathbf{G})^{-1}\mathbf{G}^H\mathbf{R}\mathbf{\Psi}$ [3],[8]. Consequently, the beamformer output $\mathbf{y} = \mathbf{W}_o^H\mathbf{x}$ may be written as $\mathbf{y} = \mathbf{W}_o^H\mathbf{x} = \mathbf{Q}^H[\mathbf{u} - \mathbf{F}^H\mathbf{v}] = \mathbf{Q}^H\mathbf{e}$, where $\mathbf{u}$, $\mathbf{v}$, and $\mathbf{e}$ are the vectors shown in the *Generalized Sidelobe Canceller (GSC)* diagram in Fig. 1:

$$\mathbf{u} = \mathbf{\Psi}^H\mathbf{x}, \quad \mathbf{v} = \mathbf{G}^H\mathbf{x}, \quad \text{and} \quad \mathbf{e} = \mathbf{u} - \mathbf{F}^H\mathbf{v}. \quad (11)$$

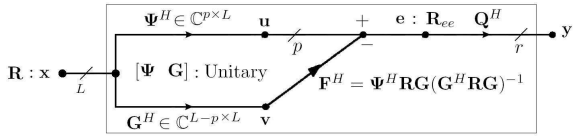

Fig. 1. Generalized sidelobe canceller (GSC).

Looking at the GSC diagram, it is easy to recognize that $\mathbf{F}^H$ is the LMMSE filter for estimating $\mathbf{u}$ from $\mathbf{v}$. Correspondingly, $\mathbf{e} = \mathbf{u} - \mathbf{F}^H\mathbf{v}$ is the error in estimating $\mathbf{u}$ from $\mathbf{v}$, with covariance [3],[8]:

$$\mathbf{R}_{ee} = E[\mathbf{e}\mathbf{e}^H] = (\mathbf{\Psi}^H\mathbf{R}^{-1}\mathbf{\Psi})^{-1}. \tag{12}$$

The power at the output of the multi-rank MVDR beamformer is given by

$$P_o = \text{tr}\{\mathbf{R}_{yy}\} = \text{tr}\{\mathbf{Q}^H\mathbf{e}\mathbf{e}^H\mathbf{Q}\} = \text{tr}\{\mathbf{Q}^H\mathbf{R}_{ee}\mathbf{Q}\}. \tag{13}$$

V. Matched Direction Beamforming versus Matched Subspace Beamforming

We now clarify how the constraint matrix $\mathbf{Q}$ should be designed in order to resolve signals of the form (3) and (5).

Referring to the data covariance $\mathbf{R}$ in (2), for the sake of simplicity and without loss of generality, let us assume that the interference covariance $\mathbf{R}_{\nu\nu}$ is rank-1 of the form $\mathbf{R}_{\nu\nu} = \sigma_\nu^2\boldsymbol{\nu}\boldsymbol{\nu}^H$, where σ_ν^2 is the interference power and $\boldsymbol{\nu}$ is its normalized signature vector. Then, we may express the error covariance matrix $\mathbf{R}_{ee} = (\mathbf{\Psi}^H\mathbf{R}^{-1}\mathbf{\Psi})^{-1}$ as

$$\mathbf{R}_{ee} = \mathbf{\Psi}^H\mathbf{R}_{ss}\mathbf{\Psi} + \sigma_\nu^2\frac{\sigma_n^2}{\sigma_n^2 + \sigma_\nu^2\boldsymbol{\nu}^H\mathbf{P}_{\mathbf{\Psi}}^{\perp}\boldsymbol{\nu}}\mathbf{\Psi}^H\boldsymbol{\nu}\boldsymbol{\nu}^H\mathbf{\Psi} + \sigma_n^2\mathbf{I}_{p\times p}, \tag{14}$$

where in obtaining (14) we have used the matrix inversion lemma twice. The first term in $\mathbf{R}_{ee}$, namely $\mathbf{\Psi}^H\mathbf{R}_{ss}\mathbf{\Psi}$, is the signal covariance matrix after it is passed through the top branch of the GSC. The second term is the covariance matrix for the interfering wavefront, after being suppressed by the GSC. The GSC reduces the interference power σ_ν^2 by a factor of $\eta^2 = \sigma_n^2/(\sigma_n^2 + \sigma_\nu^2\boldsymbol{\nu}^H\mathbf{P}_{\mathbf{\Psi}}^{\perp}\boldsymbol{\nu}) < 1$. The reduction factor η^2 is the largest when the norm of the projection $\mathbf{P}_{\mathbf{\Psi}}^{\perp}\boldsymbol{\nu}$ is close to one. This happens when the interference signature vector $\boldsymbol{\nu}$ approximately lies in $\langle\mathbf{\Psi}\rangle^{\perp} = \langle\mathbf{G}\rangle$.

The output power of the multi-rank beamformer $\mathbf{W}_o^H$ is related to the error covariance matrix $\mathbf{R}_{ee}$ as in (13). The question is how the left-orthogonal matrix $\mathbf{Q}$ should be chosen so that $\text{tr}\{\mathbf{Q}^H\mathbf{R}_{ee}\mathbf{Q}\}$ captures the signal power, for standing waves or for fluctuating waves.

A. Standing Waves and Matched Direction Beamforming

Let us first consider the case of standing waves (model (3)), where the signal covariance matrix $\mathbf{R}_{ss}$ is equal to $\mathbf{R}_{ss} = \sigma_s^2\mathbf{\Psi}\mathbf{b}_o\mathbf{b}_o^H\mathbf{\Psi}^H$ and $\mathbf{b}_o$ is an unknown but fixed orientation vector with unit norm. The error covariance $\mathbf{R}_{ee}$ is

$$\mathbf{R}_{ee} = \sigma_s^2\mathbf{b}_o\mathbf{b}_o^H + \sigma_\nu^2\frac{\sigma_n^2}{\sigma_n^2 + \sigma_\nu^2\boldsymbol{\nu}^H\mathbf{P}_{\mathbf{\Psi}}^{\perp}\boldsymbol{\nu}}\mathbf{\Psi}^H\boldsymbol{\nu}\boldsymbol{\nu}^H\mathbf{\Psi} + \sigma_n^2\mathbf{I}_{p\times p}. \tag{15}$$

When the interference term is negligible, it is the largest eigenvalue of $\mathbf{R}_{ee}$ that determines the signal power σ_s^2. Thus, to retain the signal power σ_s^2 the left-orthogonal matrix $\mathbf{Q}$ must carry the dominant eigenvector of $\mathbf{R}_{ee}$. When the interference term dominates it is not clear how the rank-1 signal term $\sigma_s^2\mathbf{b}_0\mathbf{b}_0^H$ and the rank-1 interference term $\eta^2\mathbf{\Psi}^H\boldsymbol{\nu}\boldsymbol{\nu}^H\mathbf{\Psi}$ contribute to the eigenvalues of $\mathbf{R}_{ee}$. They together determine the two largest eigenvalues of $\mathbf{R}_{ee}$. Thus, to make sure that the signal will not be suppressed, the matrix $\mathbf{Q}$ must carry the two dominant eigenvectors of $\mathbf{R}_{ee}$. The sum of the two largest eigenvalues of $\mathbf{R}_{ee}$ then captures all of the signal power. In the more general case of r_d-1 interfering terms (or an interference term with a rank-(r_d-1) covariance) the matrix $\mathbf{Q}$ must carry the r_d dominant eigenvectors of $\mathbf{R}_{ee}$ to avoid signal suppression, and the sum of the r_d largest eigenvalues of $\mathbf{R}_{ee}$ captures all of the signal power, suggesting the estimator

$$\hat{\sigma}_s^2 = \text{tr}\{\mathbf{Q}^H\mathbf{R}_{ee}\mathbf{Q}\} = \sum_{i=1}^{r_d}\text{ev}_i(\mathbf{R}_{ee}). \tag{16}$$

In summary, when the signal of interest generates standing waves (model (3)) the $p\times r_d$ constraint matrix $\mathbf{Q}$ must carry the dominant eigenvectors of the error covariance matrix $\mathbf{R}_{ee}$, to make sure that the signal is not suppressed. Here, we have used r_d in place of r to stand for matched direction. The resultant beamformer $\mathbf{W}_o^H$ may be called a *matched direction beamformer*, as it is resolves signals that are randomly drawn from an unknown direction inside a known subspace. Our use of language here is consistent with the use in [9], where matched direction detectors are derived.

B. Fluctuating Waves and Matched Subspace Beamforming

We now consider the case of fluctuating waves (model (5)), where the signal covariance $\mathbf{R}_{ss}$ is equal to $\mathbf{R}_{ss} = \sigma_s^2\mathbf{\Psi}^H\mathbf{\Lambda}\mathbf{\Psi}$. For the sake of simplicity, we consider the Slepian case, where $\mathbf{\Lambda} = \frac{1}{p}\mathbf{I}$, and hence the error covariance matrix $\mathbf{R}_{ee}$ becomes

$$\mathbf{R}_{ee} = \frac{\sigma_s^2}{p}\mathbf{I}_{p\times p} + \sigma_\nu^2\frac{\sigma_n^2}{\sigma_n^2 + \sigma_\nu^2\boldsymbol{\nu}^H\mathbf{P}_{\mathbf{\Psi}}^{\perp}\boldsymbol{\nu}}\mathbf{\Psi}^H\boldsymbol{\nu}\boldsymbol{\nu}^H\mathbf{\Psi} + \sigma_n^2\mathbf{I}_{p\times p}. \tag{17}$$

When the interference term is negligible, all the eigenvalues of $\mathbf{R}_{ee}$ are equal to $\text{ev}_i(\mathbf{R}_{ee}) = \frac{\sigma_s^2}{p} + \sigma_n^2$, $i = 1,\ldots,p$ and hence $\mathbf{Q}$ may be selected to carry any collection of r_s of the eigenvectors of $\mathbf{R}_{ee}$. An estimate of σ_s^2 is then given by $\hat{\sigma}_s^2 = \frac{p}{r_s}\text{tr}\{\mathbf{Q}^H\mathbf{R}_{ee}\mathbf{Q}\} = \sigma_s^2 + p\sigma_n^2$. When the interference term dominates, the first eigenvalue of $\mathbf{R}_{ee}$ (assuming that the eigenvalues of $\mathbf{R}_{ee}$ are arranged in descending order) is dominated by the interference. However, the rest of the eigenvalues of $\mathbf{R}_{ee}$ are all equal to $\text{ev}_i(\mathbf{R}_{ee}) = \frac{\sigma_s^2}{p} + \sigma_n^2$, $i = 2,\ldots,p$. Therefore, the $p\times r_s$ left-orthogonal matrix $\mathbf{Q}$ must be selected to carry the $r_s < p$ subdominant eigenvectors of $\mathbf{R}_{ee}$. This controls the effect of the interference term on the estimate of σ_s^2. Here, we have used r_s in place of r to stand for matched subspace.

Therefore, when the signal of interest generates fluctuating waves (model (5)) the $p\times r_s$ left-orthogonal matrix $\mathbf{Q}$ must

carry the r_s *subdominant eigenvectors* of the error covariance matrix $\mathbf{R}_{ee}$, and an estimate of the signal power is given by

$$\hat{\sigma}_s^2 = \frac{p}{r_s} P_o = \frac{p}{r_s} \mathrm{tr}\{\mathbf{Q}^H \mathbf{R}_{ee} \mathbf{Q}\} = \frac{p}{r_s} \sum_{i=p}^{p-r_s+1} \mathrm{ev}_i(\mathbf{R}_{ee}). \quad (18)$$

Since here the multi-rank MVDR beamformer $\mathbf{W}_o^H$ resolves signals that are drawn from a known multi-dimensional subspace, we call $\mathbf{W}_o^H$ a *matched subspace beamformer*. Our use of language here is consistent with the use in [10], where matched subspace detectors are derived.

VI. Discussions and numerical examples

Our goal here is to analyze the performance of matched direction and matched subspace beamformers using simple numerical examples and to illuminate the role of the eigenvalues of $\mathbf{R}_{ee}$ in resolving signals of the form (3) and (5).

We consider a ULA with $L = 128$ elements and half-wavelength inter-element spacings. Four sources of the form (3) and four sources of the form (5) are incident on the array. From here on we refer to the sources that generate standing waves as rank-1 sources. Similarly, we refer to sources that generate fluctuating waves as multi-rank sources. All sources are drawn from the $\beta L = 4$ dimensional Slepian subspace $\langle \mathbf{\Psi} \rangle$, with fractional wave-number bandwidth $\beta = 4/L$. The signal power σ_s^2 for each source and the noise power σ_n^2 at each sensor element are chosen as $\sigma_s^2 = 1$ and $\sigma_n^2 = 0.1/L$, resulting in an input SNR of 10 dB. The four rank-1 sources are centered at electrical angles 0, 1, 2.22, and 2.29 radians, and the four multi-rank sources are centered at electrical angles -2.2, -1.3, -1, and -0.49 radians. The rank-1 sources have different orientation vectors $\mathbf{b}_o$. These orientation vectors are fixed, but they are unknown to the beamformer. The orientation vectors for the multi-rank sources are randomly drawn from a distribution with covariance $\Lambda = \frac{1}{p}\mathbf{I}$.

Figures 2 (a)-(f) show the bearing response patterns for the conventional (Bartlett) and standard MVDR beamformers (Figs. 2(a),(b)), matched direction beamformers (Figs. 2(c),(d)), and matched subspace beamformers (Figs. 2(e),(f)) versus electrical angle θ. For the conventional and MVDR beamformers these plots are obtained by steering the bearing vector $\boldsymbol{\psi}(\theta)$ in electrical angle and computing the output power $P = \boldsymbol{\psi}(\theta)^H \mathbf{R} \boldsymbol{\psi}(\theta)$ (for conventional) and $P = (\boldsymbol{\psi}(\theta)^H \mathbf{R}^{-1} \boldsymbol{\psi}(\theta))^{-1}$ (for MVDR) for various electrical angles θ. For matched direction and matched subspace beamformers the plots are obtained by steering the Slepian basis $\langle \mathbf{\Psi} \rangle$ around in electrical angle and evaluating (16) and (18), with $\mathbf{R}_{ee} = (\mathbf{\Psi}(\theta)^H \mathbf{R}^{-1} \mathbf{\Psi}(\theta))^{-1}$. The steered Slepian basis $\mathbf{\Psi}(\theta)$ may be obtained by post-multiplying the broadside Slepian basis $\langle \mathbf{\Psi}(0) \rangle$ (corresponding to an angular bandwidth centered at 0 rad) by $\mathbf{D}(e^{j\theta}) = \mathrm{diag}(1, e^{j\theta}, \ldots, e^{j(L-1)\theta})$.

Referring to Figs. 2(a),(b), the conventional and MVDR beamformers fail to resolve the rank-1 sources (the conventional beamformer produces false peaks and the MVDR beamformer does not peak at all), and they render wide and flat peaks for the multi-rank sources.

The bearing response patterns for matched direction beamformers of rank one and two are plotted in Figs. 2(c),(d), which show that matched direction beamformers resolve the rank-1 sources. The bearing response patterns for matched subspace beamformers of rank one and two are given in Fig. 2(e),(f). The plots show that matched subspace beamformers resolve the multi-rank sources, rendering sharp peaks at the center of the angular bandwidth. However, they can not resolve the rank-1 sources. The reason is that the rank-1 sources contribute to the dominant eigenvalues of $\mathbf{R}_{ee}$, which are not selected in matched subspace beamforming. As can be seen the rank-2 matched subspace beamformer has a wider response than the rank-1 matched subspace beamformer. These plots verify that matched direction beamformers resolve signals of the form (3) and that matched subspace beamformers resolve signals of the form (5) and validate our designs. However they do not bring much insight about why the plots in Figs. 2(c)-(f) look the way they do. Insight may be gained by looking at the plots of the eigenvalues of the error covariance matrix $\mathbf{R}_{ee}$ versus electrical angle (eigenvalue bearing response patterns), which are shown in Figs. 2(g)-(j). In fact, as we shall discuss next it may be more interesting to use these eigenvalues instead of their averages for beamforming.

Figures 2(g)-(j) show that the dominant eigenvalue of $\mathbf{R}_{ee}$, i.e., $\mathrm{ev}_1(\mathbf{R}_{ee})$, resolves the rank-1 sources, and that the subdominant eigenvalues of $\mathbf{R}_{ee}$, say $\mathrm{ev}_4(\mathbf{R}_{ee})$ and $\mathrm{ev}_3(\mathbf{R}_{ee})$, resolve the multi-rank sources. The values of the eigenvalues of $\mathbf{R}_{ee}$ at the center of the angular bandwidth for multi-rank sources are approximately equal to $\frac{1}{p}\sigma_s^2 + \sigma_n^2 \approx -6$ dB, which is consistent with our earlier discussion. What may seem puzzling in these plots is the fact that the bearing response patterns for the dominant eigenvalues are flat in a relatively wide neighborhood around the center of the multi-rank sources, rendering poor resolution, but as we move towards the subdominant eigenvalues the bearing response patterns get narrower, rendering higher resolution. This behavior may be explained by looking at the error covariance expression in (14). For the sake of simplicity and without loss of generality, let us assume that only one source is present (interference term is negligible). Suppose the rank-p source with covariance $\mathbf{R}_{ss} = \sigma_s^2 \mathbf{\Psi}(\bar{\theta}) \mathbf{\Lambda} \mathbf{\Psi}(\bar{\theta})^H$, $\mathbf{\Lambda} = \frac{1}{p}\mathbf{I}$ is centered at electrical angle $\bar{\theta}$. When the beamforming subspace $\langle \mathbf{\Psi}(\theta) \rangle$ is steered to electrical angle θ the error covariance matrix $\mathbf{R}_{ee}$ is of the form $\mathbf{R}_{ee} = \mathbf{R}_{ee}(\theta) = \frac{\sigma_s^2}{p} \mathbf{\Psi}^H(\theta) \mathbf{P}_{\mathbf{\Psi}}(\bar{\theta}) \mathbf{\Psi}(\theta) + \sigma_n^2 \mathbf{I}$, where $\mathbf{P}_{\mathbf{\Psi}}(\bar{\theta}) = \mathbf{\Psi}(\bar{\theta}) \mathbf{\Psi}^H(\bar{\theta})$ is the orthogonal projection matrix onto the Slepian subspace $\langle \mathbf{\Psi}(\bar{\theta}) \rangle$. The first term in $\mathbf{R}_{ee}$ depends on the location of the source $\bar{\theta}$ and the electrical angle θ for beamforming, which we sweep over. Let β be the fractional wave-number bandwidth for the Slepian subspace $\langle \mathbf{\Psi}(\theta) \rangle$ and note that β is independent of the steering angle θ. When θ is far from $\bar{\theta}$ such that the angular bandwidth $[\theta - \beta\pi, \theta + \beta\pi]$ for $\langle \mathbf{\Psi}(\theta) \rangle$ and $[\bar{\theta} - \beta\pi, \bar{\theta} + \beta\pi]$ for $\langle \mathbf{\Psi}(\bar{\theta}) \rangle$ overlap only in a small fraction of $2\beta\pi$, the numerical rank of $\mathbf{\Psi}(\theta)^H \mathbf{P}_{\mathbf{\Psi}}(\bar{\theta}) \mathbf{\Psi}(\theta)$ is small. Consequently, the subdominant eigenvalues of $\mathbf{\Psi}(\theta)^H \mathbf{P}_{\mathbf{\Psi}}(\bar{\theta}) \mathbf{\Psi}(\theta)$ will be close to zero. This

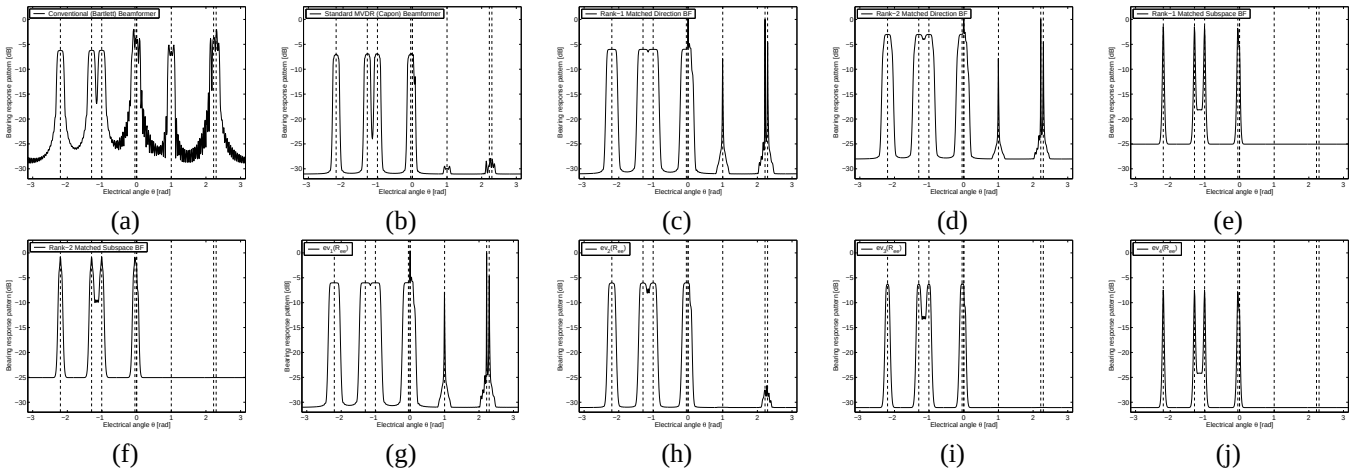

Fig. 2. Bearing response patterns for (a) conventional (Bartlett) beamformer, (b) standard MVDR beamformer, (c) rank-1 matched direction beamformer, (d) rank-2 matched direction beamformer, (e) rank-1 matched subspace beamformer, (f) rank-2 matched subspace beamformer, (g) $\text{ev}_1(\mathbf{R}_{ee})$, (h) $\text{ev}_2(\mathbf{R}_{ee})$, (i) $\text{ev}_3(\mathbf{R}_{ee})$, and (j) $\text{ev}_4(\mathbf{R}_{ee})$. Reading from left to right in each plot the first four sources generate fluctuating waves with rank-4 covariances and the next four sources generate standing waves with rank-1 covariances. The theoretical data covariance matrix $\mathbf{R}$ is assumed to be known.

explains why the bearing response pattern for the most sub-dominant eigenvalue of $\mathbf{R}_{ee}$ (Fig. 2(j)) has sharp peaks around the multi-rank sources. As θ gets closer to $\overline{\theta}$ the two angular bandwidths overlap in a wider region and hence the numerical rank of $\mathbf{\Psi}(\theta)^H\mathbf{P}_{\mathbf{\Psi}}(\overline{\theta})\mathbf{\Psi}(\theta)$ increases. Consequently, as we go towards the dominant eigenvalues of $\mathbf{\Psi}(\theta)^H\mathbf{P}_{\mathbf{\Psi}}(\overline{\theta})\mathbf{\Psi}(\theta)$ the range of electrical angles over which these eigenvalues are nonzero gets wider and wider. Thus, the most dominant eigenvalue of $\mathbf{\Psi}(\theta)^H\mathbf{P}_{\mathbf{\Psi}}(\overline{\theta})\mathbf{\Psi}(\theta)$ remains non-zero over an angular bandwidth of $4\beta\pi$ around the center of the multi-rank source. When the two-angular bandwidths stop overlapping, the numerical rank of $\mathbf{\Psi}(\theta)^H\mathbf{P}_{\mathbf{\Psi}}(\overline{\theta})\mathbf{\Psi}(\theta)$ becomes zero and the eigenvalues of $\mathbf{R}_{ee}$ collapse to σ_n^2.

The plots in Figs. 2(g)-(j) also show that averaging the eigenvalues will result in wider peaks around the center location of the sources and hence loss of "resolution", which explains why the plots in Figs. 2(c)-(f) for matched direction and matched subspace beamformers become wider with increase in the beamformer rank. Averaging the eigenvalues of $\mathbf{R}_{ee}$ may be viewed as a diversity combining technique, where *per mode (subspace dimension) powers* given by the eigenvalues are averaged to yield an estimate of the signal power. Correspondingly, the number of eigenvalues averaged may be viewed as the diversity gain. Therefore, there is a trade-off between the diversity gain and "resolution".

VII. Conclusions

We have derived two multi-rank generalizations of the MVDR beamformer; a matched direction beamformer, for the case where the signal of interest is drawn from an unknown but fixed direction within a known multi-dimensional subspace and has a rank-1 covariance matrix, and a matched subspace beamformer, for the case where the signal of interest is drawn from a known multi-dimensional subspace and has a multi-rank covariance matrix. Evidently, matched direction and matched subspace beamformers are eigenvalue beamformers that depend on an error covariance or beamformed covariance matrix.

Acknowledgment

This work is supported in part under ONR contracts N00014-04-1-0084 and N0014-00-C-0145, DARPA contracts FA9550-04-1-0371 and FA8750-05-2-0285, and NIH award 1R21EB005473.

References

[1] H. L. Van Trees, *Optimum Array Processing.* Wiley Interscience, 2002.
[2] J. Li and P. Stoica, *Robust Adaptive Beamforming.* Wiley, 2005.
[3] A. Pezeshki, B. D. Van Veen, L. L. Scharf, H. Cox, and M. Lundberg, "Eigenvalue beamforming using a multi-rank MVDR beamformer and subspace selection," submitted to *IEEE Trans. Signal Process.*
[4] D. Slepian, "Prolate spheroidal wave functions, Fourier analysis and uncertainty - V: The discrete case," *Bell Syst. Tech. J.*, pp. 1371–1430, 1978.
[5] H. Cox, "Sensitivity considerations in adaptive beamforming," in *Signal Processing (Proc. NATO Advanced Study Inst. Signal Processing with Particular Reference to Underwater Acoust., Loughborough, U.K., Aug. 1972)*, J. W. R. Griffiths, P. L. Stocklin, and C. Van Schooneveld, Eds. New York and London: Academic, 1973, pp. 619–645.
[6] T.-C. Lui and B. D. Van Veen, "Multiple window based minimum variance spectrum estimation for multidimensional random fields," *IEEE Trans. Signal Process.*, vol. 40, pp. 578–589, Mar. 1992.
[7] B. D. Van Veen, W. van Drongelen, M. Yuchtman, and A. Suzuki, "Localization of brain electrical activity via linearly constrained minimum variance spatial filtering," *IEEE Trans. Biomed. Eng.*, vol. 44, pp. 867–880, Sept. 1997.
[8] A. Pezeshki, L. L. Scharf, M. Lundberg, and E. K. P. Chong, "Constrained quadratic minimizations for signal processing and communications," in *Proc. Forty-Fourth IEEE Conf. Decision Contr.*, Seville, Spain, Dec. 2005, pp. 7949–7953.
[9] O. Besson, L. L. Scharf, and F. Vincent, "Matched direction detectors and estimators for array processing with subspace steering vector uncertainties," *IEEE Trans. Signal Process.*, vol. 53, pp. 4453–4463, Dec. 2005.
[10] L. L. Scharf and B. Friedlander, "Matched subspace detectors," *IEEE Trans. Signal Process.*, vol. 42, pp. 2146–2157, Aug. 1994.